A New Strategy to Extend the Speed Range in a Permanent Magnet AC Motor

Roberto Leidhold[1], Guillermo Bossio[2], Guillermo García[3] and María Inés Valla[4]

[1, 2, 3] Grupo de Electrónica Aplicada (GEA), Universidad Nacional de Río Cuarto
Ruta Nacional #36, Km. 601, (5800) Río Cuarto, Córdoba, Argentina
rleidhold@ieee.org, g.garcia@ieee.org, gbossio@ing.unrc.edu.ar

[4] Laboratorio de Electrónica Industrial, Control e Instrumentación (LEICI)
Facultad de Ingeniería, Universidad Nacional de La Plata
CC 91, 1900 La Plata, Argentina
m.i.valla@ieee.org

***Abstract*—A new online speed extension strategy for sinusoidal and non sinusoidal (i.e. trapezoidal) EMF waveform Permanent Magnet AC Motors (PMACM) is presented. This strategy is based on the instantaneous active and reactive power theory. It can be implemented disregarding which torque control algorithm is used, and it is decoupled from torque production. A non-sinusoidal EMF waveform PMACM model is presented in order to analyze how reactive current affects the stator voltage and to deduce the corresponding algorithm. Simulation results are presented in order to show the algorithm feasibility.**

I. INTRODUCTION

Modern high-energy permanent-magnet materials, as Neodymium-iron-boron (NdFeB) and samarium-cobalt (SmCo), make possible the development of Permanent Magnet AC Motors (PMACM) with very high power density and very high efficiency. PMACM are being used mainly in high-performance motion control applications (e.g. industrial and electrical traction drives). The PMACM is characterized for having constant flux, therefore its maximum torque is determined by the maximum allowed current. The inverter can supply current if the EMF is lower than the maximum inverter voltage. Therefore, as the EMF is proportional to the speed, the maximum speed at which the machine can produce torque is bounded. However, the stator-inductance voltage-drop vector can be modified by supplying reactive current, in order to reduce the stator voltage, allowing a higher maximum speed. As a drawback, more current is required for the same torque at lower speeds. Although this technique is usually known as Flux-Weakening it is different as the applied to Induction, DC and Synchronous Machines.

PMACM can be divided into two types [1]:

- Sinusoidal PMACM and
- Trapezoidal PMACM.

Sinusoidal PMACM derive from the conventional synchronous machines, where the rotor excitation-winding is replaced by a PM-rotor and both the air-gap magneto-motive force (MMF) and the back-electro-motive force (EMF) are sinusoidal. In this case the conventional field orientation (i.e. rotor orientation) is used [2], where direct (d-axis) and quadrature (q-axis) currents are controlled. The q-axis current is used for torque control and the d-axis current for reactive current supplying.

Trapezoidal machine derives from the Permanent Magnet DC Machines, where the mechanical commutator is replaced by an electronic commutator. These machines usually have a rectangular air-gap MMF and concentrated windings. Concentrated windings are of simpler construction than those sinusoidally distributed, allowing the arrangement of a higher pole-number. In this case, the back-EMF waveform is ideally trapezoidal. This machines are usually controlled by exciting them with a six-step switched current waveform [1] or a programmed current waveform (e.g. [3]-[6]). The torque is controlled by the current waveform amplitude, and the reactive current is supplied by leading the current. However, as in non-sinusoidal machines current leading produce active current harmonics in addition to the reactive current, undesired torque effects will be produced.

The most common control for either d-axis current or current leading is by a feedforward scheme. In this schemes the control variable is calculated offline considering the mathematical model and its parameters (e.g. [7] and [8]) or based on experimentation [9]. However some proposals of online d-axis current or current leading control algorithm were presented in the literature (e.g. [10] and [11]).

In this work a new online algorithm to extend the speed range of a PMACM drive is proposed. This algorithm is based on the instantaneous active and reactive power theory [12]. The algorithm controls the reactive current in order to reduce the stator voltage. This is achieved decoupled from the torque production and without concerning the EMF waveform and the torque control algorithm.

This work is organized as follows: in section II the instantaneous active and reactive power definitions are presented; in section III a non-sinusoidal PMACM model is presented; in section IV the speed range extension algorithm is presented; in section V some simulation results are presented; finally, in section VI some conclusions are drawn.

II. Instantaneous Active and Reactive Power Definitions.

As it was stated in the introduction, the control strategy is based on the instantaneous active and reactive power theory. Therefore some definitions and transformations, that will be used later, are outlined here.

In order to analyze the instantaneous active and reactive power, the $\alpha-\beta$ transformation, also called Clarke transformation, is used. This transformation, for a generic magnitude, is given by,

$$\begin{bmatrix} f_\alpha \\ f_\beta \end{bmatrix} = K \begin{bmatrix} f_a \\ f_b \\ f_c \end{bmatrix}, \tag{1}$$

where,

$$K = \sqrt{\frac{2}{3}} \begin{bmatrix} 1 & -1/2 & -1/2 \\ 0 & \sqrt{3}/2 & -\sqrt{3}/2 \end{bmatrix}, \tag{2}$$

f is a generic variable as current, voltage or flux. The considered machines are of the three-phase three-wire type, therefore there is no zero-sequence components.

The instantaneous active (p) and reactive (q) power are defined as follows [12],

$$p = u_\alpha\, i_\alpha + u_\beta\, i_\beta\ , \tag{3}$$

$$q = u_\alpha\, i_\beta - u_\beta\, i_\alpha\ , \tag{4}$$

where u and i represent the voltages and currents at a given section of a three phase system. Subscripts α and β denotes the direct and quadrature axis, respectively, related with an arbitrary reference frame (e.g stationary) [13]. It is important to emphasize that the value of p and q are independent of the defined reference frame.

Knowing the instantaneous active and reactive powers and voltages, the corresponding currents can be deduced from (3)-(4), as follows,

$$i_\alpha = \frac{p\, u_\alpha - q\, u_\beta}{u_\alpha^2 + u_\beta^2}\ , \tag{5}$$

$$i_\beta = \frac{p\, u_\beta + q\, u_\alpha}{u_\alpha^2 + u_\beta^2}\ . \tag{6}$$

A particular reference frame, that is useful to analyze the instantaneous active and reactive power, is the one oriented by the voltage. Using this reference frame, the direct and quadrature components of voltage are,

$$u_d = 0\ , \tag{7}$$

$$u_q = |u| = \sqrt{u_\alpha^2 + u_\beta^2}\ . \tag{8}$$

Substituting current subscripts α and β by q and d, respectively, and plugging (7) and (8) into (5) and (6), yields to,

$$i_q = \frac{p}{|u|} \tag{9}$$

$$i_d = \frac{q}{|u|} \tag{10}$$

where i_q, named active current, is the component that transmits only active power to the load side; and i_d, called reactive current, does not transmit any active power.

III. PMACM Model

If saliences are negligible, the PMACM can be modeled in the $\alpha-\beta$ coordinates as shown in the following equations,

$$\begin{aligned} v_\alpha &= i_\alpha\, R_s + \frac{d\, i_\alpha}{d\, t} L_s + e_\alpha \\ v_\beta &= i_\beta\, R_s + \frac{d\, i_\beta}{d\, t} L_s + e_\beta \end{aligned}\ , \tag{11}$$

where v is the stator voltage, i is the stator current, e is the back-EMF, R_s is the stator resistance and L_s is the stator inductance.

From equations (11), the PMACM equivalent circuit shown in Fig. 1 can be deduced. As the flux linkage depends only on the position of the permanent magnet, fixed to the rotor, the corresponding back-EMF induced in the stator can be expressed in terms of the rotor position and speed, as follows,

$$\begin{aligned} e_\alpha &= \frac{d\,\lambda_\alpha}{dt} = \frac{\partial\,\lambda_\alpha}{\partial\theta}\,\omega = \varphi_\alpha(\theta)\,\omega \\ e_\beta &= \frac{d\,\lambda_\beta}{dt} = \frac{\partial\,\lambda_\beta}{\partial\theta}\,\omega = \varphi_\beta(\theta)\,\omega \end{aligned}\ , \tag{12}$$

where λ is the flux linkage, θ is the rotor position and,

$$\omega = \frac{d\,\theta}{dt}\ , \tag{13}$$

The derivative of the flux linkage with respect to its angular position can be obtained by measuring the instantaneous stator voltages, rotor position and speed at a no-load test.

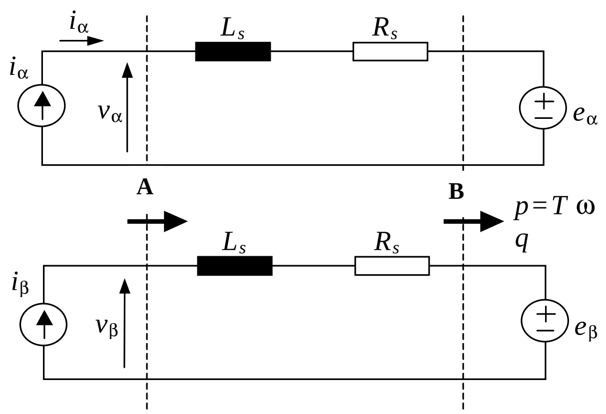

Fig. 1. PMACM equivalent circuit in α-β coordinates.

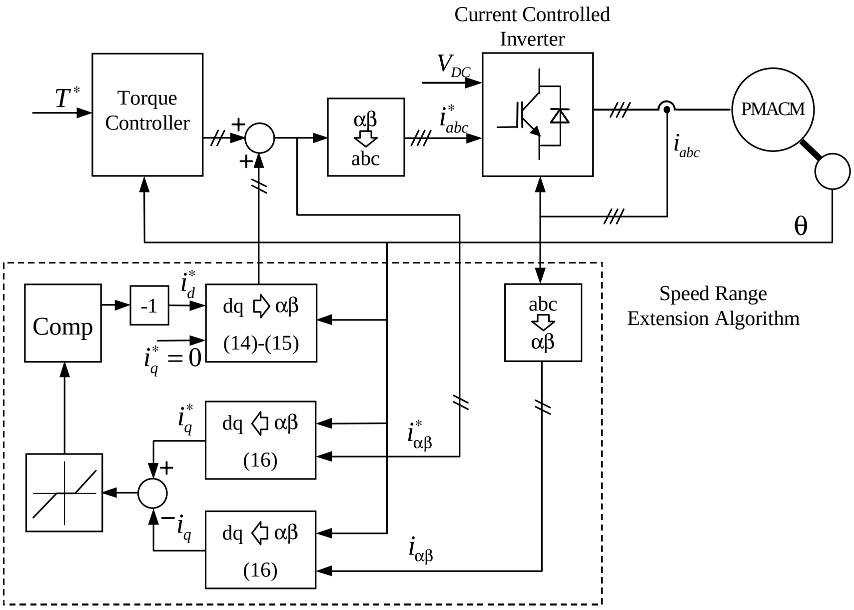

Fig. 2. Simplified block-diagram of the proposed speed range extension algorithm.

In Fig. 1 two sections of the machine are considered for instantaneous active and reactive power analysis. Power p and q in section A correspond to the stator-inverter link, while power p and q in section B correspond to the airgap. That means that p is the electromechanical power (i.e. torque times speed) while q does not affect the output torque. However as will be shown later, the reactive power (i.e. reactive current) will affect the stator voltage, and can therefore be used for speed range extension without affecting the output torque.

As stated in the preceding section, the voltage-oriented reference frame will be useful for instantaneous active and reactive power analysis. Moreover, as section B of Fig. 1 is the one of interest for the PMACM analysis, the voltage at this section (i.e. the EMF, e or φ) will be the used as reference frame.

The $d-q$ to $\alpha-\beta$ transformation can be obtained by combining (9)-(10) with (5)-(6) and substituting u by the EMF expression (12), yielding,

$$i_\alpha = \frac{i_q\,\varphi_\alpha - i_d\,\varphi_\beta}{|\varphi|}, \tag{14}$$

$$i_\beta = \frac{i_q\,\varphi_\beta + i_d\,\varphi_\alpha}{|\varphi|}, \tag{15}$$

and the inverse transformation is,

$$i_q = \frac{i_\alpha\,\varphi_\alpha + i_\beta\,\varphi_\beta}{|\varphi|}, \tag{16}$$

$$i_d = \frac{i_\beta\,\varphi_\alpha - i_\alpha\,\varphi_\beta}{|\varphi|}. \tag{17}$$

The PMACM model (11) can be expressed oriented by the EMF applying the transformation (16) and (17), yielding,

$$\begin{aligned} v_q &= R_s\,i_q + L_s\frac{d\,i_q}{d\,t} + \omega|\varphi(\theta)| + L_s\,\omega i_d\,F(\theta) \\ v_d &= R_s\,i_d + L_s\frac{d\,i_d}{d\,t} - L_s\,\omega i_q\,F(\theta) \end{aligned}, \tag{18}$$

where,

$$F(\theta) = \frac{\varphi_\beta(\theta)\dfrac{d\,\varphi_\alpha(\theta)}{d\,\theta} - \varphi_\alpha(\theta)\dfrac{d\,\varphi_\beta(\theta)}{d\,\theta}}{\varphi_\alpha^2(\theta) + \varphi_\beta^2(\theta)}, \tag{19}$$

In the case that the PMACM has sinusoidal EMF distribution, i.e. $\varphi_\alpha(\theta) = |\varphi|\sin(\theta)$ and $\varphi_\beta(\theta) = |\varphi|\cos(\theta)$, the equation (19) is $F(\theta) = 1$.

It can be seen in (18) that the q axis stator voltage depends mainly on the speed and the reactive current, while the d axis stator voltage depends mainly on the active current.

IV. Proposed Algorithm

Independently of the torque-control strategy and the EMF waveform, the instantaneous reactive power theory gives a method to supply reactive current which affect the stator voltage as shown in equation (18) and without affecting the generated torque.

When the PMACM speed is low, the stator voltage is lower than the maximal voltage the inverter can feed and the current controller will work properly. On the other hand, when the speed grows, the stator voltage can grow beyond the maximum inverter voltage and the current controller saturates. In this case, supplying negative reactive current will reduce the stator voltage, as can be seen in (18).

A generalized PMACM drive for torque control, and the proposed algorithm, is shown in Fig. 2.

In this figure the PMACM is connected to a Current Controlled Inverter. Based on the measured rotor position and on the torque reference, a Torque Controller generates the $\alpha\beta$ current references. This references converted to *abc* variables are the Current Controlled Inverter references. This is a generalized scheme of a torque controlled PMACM drive.

In the same figure within the dashed box, the proposed algorithm is shown. First, the reference currents in $\alpha\beta$ are sampled and the actual currents are sampled and converted to $\alpha\beta$. This currents are converted to the qd reference frame using equation (16) and the reference and actual active currents are compared to detect the Current Controller saturation [10]. Some minimal active current error have to be admitted due to the normal inverter operation, therefore the active current error is connected to a dead zone block. The dead zone block output is connected to a lag compensator whose output is the negative reactive current reference. The reactive current reference is converted to the $\alpha\beta$ reference frame by using equation (14) and (15) and, finally, they are added to the torque controller current references.

V. Simulation and Experimental Results

In this section, experimental and simulation results are presented in order to validate the proposed algorithm. The motor parameters are shown in Table I.

In Fig. 3, Fig. 4 and Fig. 5 the functions $\{\varphi_a(\theta), \varphi_b(\theta), \varphi_c(\theta)\}$, $\{\varphi_\alpha(\theta), \varphi_\beta(\theta)\}$ and $F(\theta)$ respectively are shown, where θ is expressed in electrical radians.

A. Simulation Results

The PMACM simulation model is implemented with equations (15)-(17). The current controlled inverter is modeled considering a 10 (kHz) switching frequency delta modulation. The torque control used in the simulation is an algorithm to minimize the ripple torque, as proposed by [6].

TABLE I
PMACM Drive Parameters

Parameter	Value
Nominal Current	23 A
Torque Constant	0.826 Nm/A
FEM Constant	54.6 V/Krpm
Pole pair	4
R	0.1 Ω
L	8 mH
V_{DC}	100 V

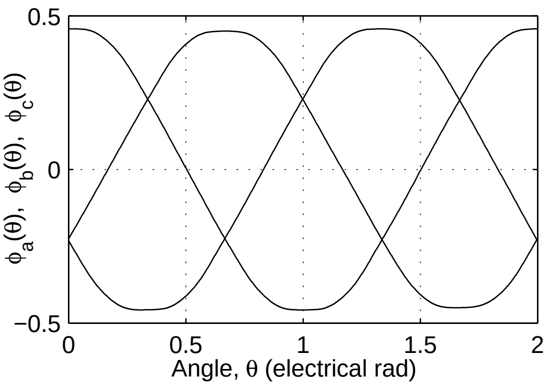

Fig. 3. PMACM flux linkage derivative with respect to its angular position in *abc* variables.

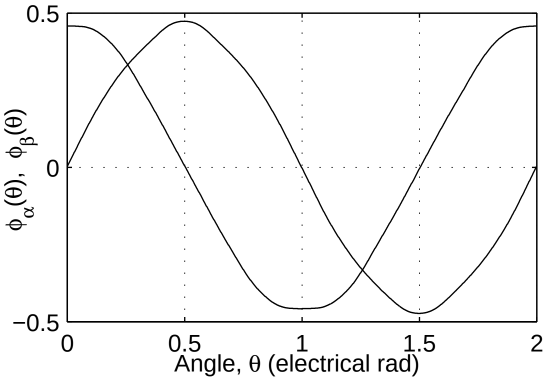

Fig. 4. PMACM flux linkage derivative with respect to its angular position in $\alpha\beta$ variables.

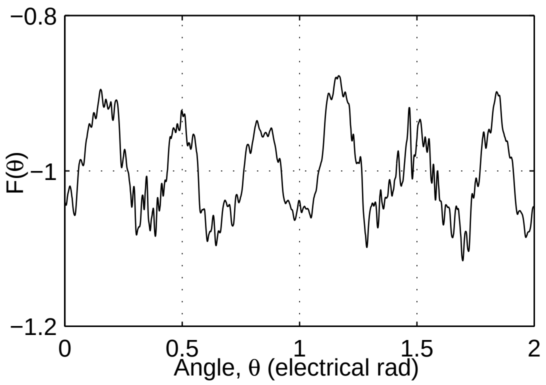

Fig. 5. PMACM $F(\theta)$ function.

For testing the torque-speed behavior the machine is started up from standstill with constant torque reference. The torque value is the machine nominal torque. The machine has a high inertia load in order to have a low speed slope.

Figure 6 shows the PMACM drive behavior when the reactive current reference is zero (e.g. without the speed extension algorithm). In this figure the torque, active current reference and the actual active current are shown as function of the speed. It can be seen that beyond the nominal speed (900 rpm), the inverter become saturated resulting in a high active current error, and torque decrease.

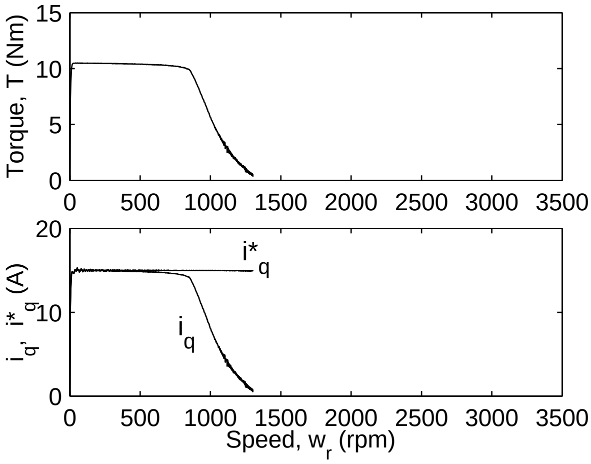

Fig. 6. PMACM drive behavior when the reactive current reference is zero (e.g. without the speed extension algorithm).

Figure 7 shows the PMACM drive behavior with the proposed speed extension algorithm. In this figure the torque, active current reference, actual active current and the algorithm generated reactive current are shown as function of the speed. Here when the speed raises beyond the nominal speed, the proposed algorithm detects the active current error and supplies reactive current in order to reduce it. Simultaneously while the reactive current increases, the active current upper limit is reduced in order to restrain the current amplitude.

With the particular PMACM described, the proposed speed extension algorithm allowed to obtain speeds approximately three times the nominal speed. Higher speeds may be obtained by temporarily increasing the stator current.

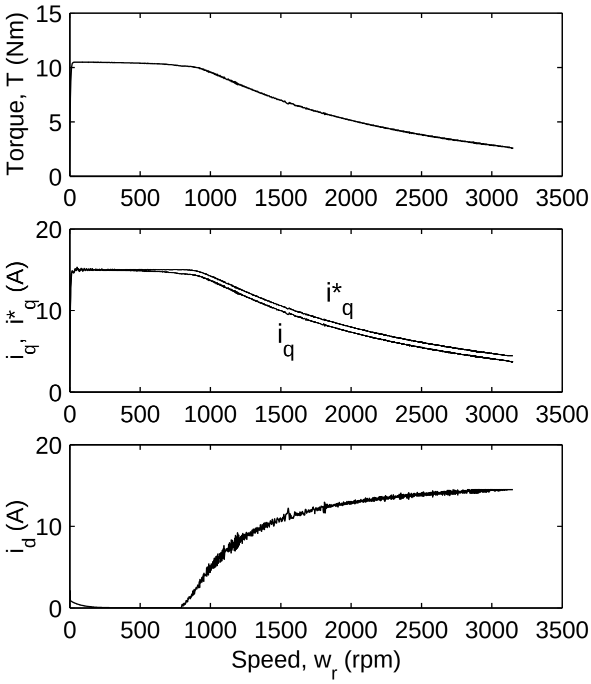

Fig. 7. PMACM drive behavior with the proposed speed extension algorithm.

B. Experimental Results

The PMACM experimental results were obtained using the above described motor mechanically connected to a eddy-current brake. The motor is driven by an IGBT current controlled inverter. The torque control algorithm and the speed extension strategy was implemented using an Pentium PC with an adequate interface.

In Fig. 8 the experimental PMAC drive behavior without the speed extension strategy is shown.

Figure 9 shows the experimental PMACM drive behavior using the proposed speed extension algorithm.

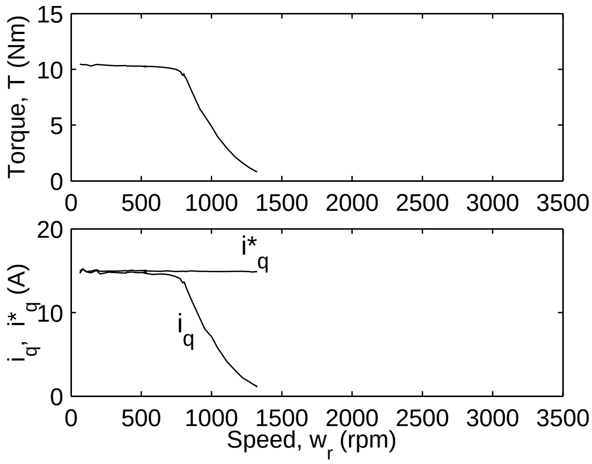

Fig. 8. Experimental PMACM drive behavior without the speed extension strategy.

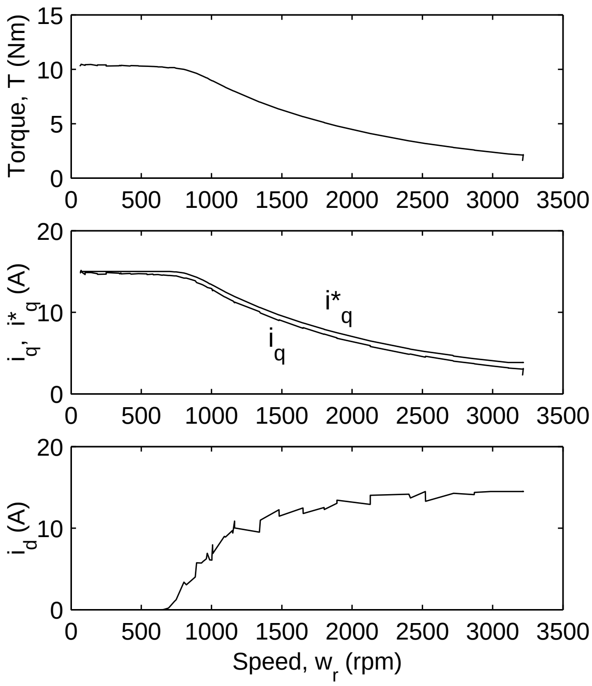

Fig. 9. experimental PMACM drive behavior with the proposed speed extension algorithm.

VI. Conclusions

In this work an algorithm for PMACM speed range extension was proposed. In order to analyze how reactive current affect the stator voltage, a generalized (non-sinusoidal) PMACM model in a EMF oriented reference frame was presented. By using the active and reactive instantaneous power concepts, it was possible to supply a reactive current without disturbing the generated torque and without concerning the EMF waveform nor the used torque control algorithm.

This algorithm supplies a reactive current to the PMACM which reduces the stator voltage, allowing a higher speed limit. The reactive current magnitude is determined online by a lag compensator whose input is the inverter active current error.

A complete simulation model was implemented and some simulation results were presented in order to show the feasibility of the proposed algorithm. The same tests driven by simulation were carried out experimentally. This results shows high agreement to the obtained by simulation.

VII. Acknowledgment

The authors wish to acknowledge the financial support and motivation provided by Universidad Nacional de Río Cuarto (UNRC), ANPCyT, CONICET and the WEG Company.

VIII. References

[1] T.M. Jahns, "Variable Frequency Permanent Magnet AC Machine Drives". In: *Power Electronics and Variable Frequency Drives* (Edited by Bimal K. Bose) IEEE Press, New York, 1997, pp. 277-331.

[2] W. Leonhard, *Control of Electrical Drives*, Springer-Verlag Berlin Heidelberg, 1996.

[3] H. Le-Huy, R. Perret and R. Feuillet, “Minimization of Torque Ripple in Brushless DC Motor Drives”, *IEEE Trans. on Industry Application*, vol. 22, no. 4, pp. 748-755, Jul./Aug. 1986.

[4] D.C. Hanselman, “Minimum torque ripple, maximum efficiency excitation of brushless permanent magnet motors”, *IEEE Trans. on Industrial Electronics*, vol. 41, no. 3, pp. 292-300, June 1994.

[5] T.M. Jahns, W.L. Soong, “Pulsating torque minimization techniques for permanent magnet AC motor drives-a review”, *IEEE Trans. on Industrial Electronics*, vol. 43, no. 2, pp. 321-330, April 1996.

[6] R. Leidhold, G. García and E. Watanabe, “PMAC Motor Control Strategy, Based on the Instantaneous Active and Reactive Power, for Ripple-Torque and Copper-Losses Minimization”, *IEEE-IECON-2000*. Oct. 2000.

[7] S. Morimoto, M. Sanada, Y. Takeda, “Wide-speed operation of interior permanent magnet synchronous motors with high-performance current regulator”, *IEEE Trans. on Industry Applications*. vol. 30, no. 4, pp. 920-926, July/Aug. 1994.

[8] T.M. Jahns, “Flux-Weakening Regime Operation of an Interior Permanent-Magnet Syncronous Motor Drive” *IEEE Trans. on Industry Aplications*, vol. 23, no. 4, pp. 681-689, 1987.

[9] C.C. Chan, J.Z. Jiang, W. Xia, K.T. Chan, “Novel wide range speed control of permanent magnet brushless motor drives”, *IEEE Trans. on Power Electronics*, vol. 10, no. 5, pp. 539-546, Sep. 1995.

[10] Z. Q. Zhu, Y. S. Chen and D. Howe, “Online Optimal Flux-Weakening Control of Permanent-Magnet Brushless AC Drives”, *IEEE Trans. On Industry Applications*, vol. 36, no. 6, pp. 1661-1668, Nov./Dec. 2000.

[11] R. Leidhold, G. García, G. Bossio y M. I. Valla, "Control para la Extensión del rango de velocidad en Máquinas de C.A. de Imanes Permanentes". *XVII Congreso Argentino de Control Automático* (AADECA 2000), Vol. 1, pp 263-268. Sep. 2000.

[12] H. Akagi, Y. Kanazawa and A. Nabae, “Generalized Theory of the Instantaneous Reactive Power in Three-Phase Circuits.” *IEEE - IPEC 83* - pp. 1375.

[13] P. Krause and O. Wasynczuk, *Analysis of Electric Machinery*, IEEE Press, 1994.